JACS
JOURNAL OF THE AMERICAN CHEMICAL SOCIETY

ARTICLE

pubs.acs.org/JACS

The Role of Water H-Bond Imbalances in B-DNA Substate Transitions and Peptide Recognition Revealed by Time-Resolved FTIR Spectroscopy

Hassan Khesbak, Olesya Savchuk, Satoru Tsushima, and Karim Fahmy*

Division of Biophysics, Instititute of Radiochemistry, Helmholtz-Zentrum Dresden-Rossendorf, D-01314 Dresden, PF 510119, Germany

ABSTRACT: The conformational substates B_I and B_{II} of the phosphodiester backbone in B-DNA are thought to contribute to DNA flexibility and protein recognition. We have studied by rapid scan FTIR spectroscopy the isothermal B_I-B_{II} transition on its intrinsic time scale. Correlation analysis of IR absorption changes occurring within seconds after a reversible incremental growth of the DNA hydration shell identifies water populations w_1 (PO_2^--bound) and w_2 (non-PO_2^--bound) exhibiting weaker and stronger H-bonds, respectively, than those dominating in bulk water. The B_{II} substate is stabilized by w_2. The water H-bond imbalance of 3−4 kJ mol^{-1} is equalized at little enthalpic cost upon formation of a contiguous water network (at 12−14 H_2O molecules per DNA phosphate) of reduced ν(OH) bandwidth. In this state, hydration water cooperatively stabilizes the B_I conformer via the entropically favored replacement of w_2−DNA interactions by additional w_2−water contacts, rather than binding to B_I-specific hydration sites. Such water rearrangements contribute to the recognition of DNA by indolicidin, an antimicrobial 13-mer peptide from bovine neutrophils which, despite little intrinsic structure, preferentially binds to the B_I conformer in a water-mediated induced fit. The FTIR spectra resolve sequential steps leading from PO_2^--solvation to substate transition and eventually to base stacking changes in the complex. In combination with CD-spectral titrations, the data indicate that, in the absence of a bulk aqueous phase, as in molecular crowded environments, water relocation within the DNA hydration shell allows for entropic contributions similar to those assigned to water upon DNA ligand recognition in solution.

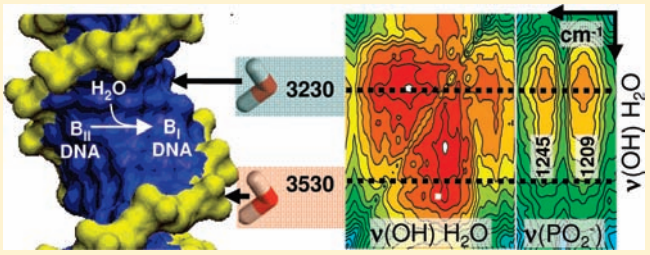

INTRODUCTION

The ubiquitous presence of water in biological systems renders the hydration shell (HS), a constitutive component in biomolecular structure. This is particularly pronounced for DNA which undergoes hydration-induced transitions between A-, B-, and Z-forms[1] which have been studied extensively as reviewed.[2,3] For the biologically prevalent B-DNA, a quasi stoichiometric association of water has been deduced from calorimetry.[4] The much more subtle structural differences between B_I and B_{II} substates within the same structural class have attracted attention as they are governed by HS properties, depend on DNA methylation,[5] and may allow induced fit mechanisms in DNA recognition.[6] The two states differ in the dihedral angles around the C3′−O3′−P bonds.[7−9] Initially described for crystallized synthetic dsDNA,[10] these substates have been correlated with infrared absorption spectra[11] and their temperature-dependent interconversion has been shown also in genomic DNA from salmon testes.[6,12] Fourier transform infrared (FTIR) spectra of slow isothermal relaxations of DNA at ∼200 K suggested the migration of water from the ionic phosphates to the phosphodiester and sugar moieties during B_{II} formation in a glassy state.[6] It has remained a challenge, however, to monitor the coupling of water to the $B_{II}-B_I$ interconversion on its intrinsic time scale independently of a glass transition in the surrounding matrix and to identify distinct water populations that may link the local DNA backbone conformation to the H-bond network of the HS. Such a linkage is expected to be crucial for indirect readout mechanisms,[13−15] which rely on water-mediated DNA protein contacts and solvation-dependent parameters such as backbone flexibility and bendability.[16] Molecular dynamics calculations predict that the B_I-B_{II} transition participates in these mechanisms.[17] The femtosecond to nanosecond dynamics of DNA-bound water, as studied for example by neutron scattering[18] and fluorescence spectroscopy,[19] revealed DNA-bound water populations of different mobility but their potential association with the B_I-B_{II} transition and ligand interactions is not yet understood. For example, the structural consequences of DNA-binding peptides range from allosteric regulation of recognition sites[20] to DNA condensation[21] and both processes have a major impact on local hydration patterns. It is thus of fundamental interest to understand how the HS couples to B-DNA substate transitions and how water heterogeneity contributes to substate-specific DNA recognition by ligands that by themselves exhibit little intrinsic structure. In addition to the fine-tuning of protein recognition,[22,23] hydration-driven structural changes in DNA have recently gained further attention for the generation of responsive biomaterials.[24]

Here, we introduce a novel label-free technique that extends the potential of infrared spectroscopy to elucidate water-dependent molecular contacts in DNA ligand interactions, which may help in the rational design of DNA-targeting drugs. In essence,

Received: October 1, 2010
Published: March 29, 2011

dx.doi.org/10.1021/ja108863v | J. Am. Chem. Soc. 2011, 133, 5834–5842

the similarity or dissimilarity in the kinetic behavior of transient IR-absorption changes is exploited to distinguish potential H-bond donor/acceptor pairs from disjunct chemical groups. We use this approach to investigate the role of water heterogeneity in DNA substate conformation and peptide recognition by monitoring the $B_{II}-B_I$ transition and its relaxation within seconds after a brief hydration pulse. In contrast to freeze-trapped DNA, the B_I-B_{II} transition is found here not to be coupled to base stacking alterations. Instead, two water populations with H-bond energies slightly above and below that of bulk water merge into a contiguous nonrandom H-bond network in an entropically favorable way that links HS growth to B_I state formation. This linkage is disrupted by indolicidin, an antibacterial DNA-binding peptide expressed in bovine neutrophils.[25] Rather than exhibiting by itself a strong structural preference, the peptide relocates water in a substate-specific manner almost indistinguishable from that observed for the minor groove binder netropsin. DNA−water interactions can thus be recruited to promote ligand-dependent transitions in DNA leading in a sequential process from DNA backbone hydration to base unstacking.

MATERIALS AND METHODS

Sample Preparation. Genomic DNA from salmon testes (CALBIOCHEM) was dialyzed against Millipore water resulting in a Na/P ratio of 1.4 and negligible amounts of Ca^{2+} and Mg^{2+} as determined by inductively coupled plasma mass spectrometry using an ICP-MS-ELAN 9000 spectrometer (PerkinElmer SCIEX, Rodgau-Jügesheim, Germany). Nonoriented DNA films were obtained by drying 40 nmol (in phosphate) of DNA on a 5 mm diameter diamond attenuated-total-reflectance-(ATR)-crystal (RESULTEC, Illenkirchberg, Germany). Alternatively, HPLC-purified, trifluoroacetate-free bovine indolicidin of the sequence: ILPWKWPWWPWRR (Thermo Scientific Ulm, Germany) or the minor groove binder netropsin (Sigma-Aldrich, Seelze, Germany) was added to ~5 μL of the DNA stock solution, to achieve peptide/phosphate ratios of 1:56.

FTIR and CD Spectroscopy. A dialysis membrane placed 1 mm above the DNA films on the ATR-crystal was overlaid with 1 mL of saturated salt solutions (KNO_3, KCl, NaCl, $NaNO_2$, $Mg(NO_3)_2$, $MgCl_2$, covering 93−33% relative humidity[26]). The actual ratio Γ = mol H_2O/mol P was calculated from the water ν(OH) and the asymmetric PO_2^- stretching (PO_{as}) band[27] taking the wavelength-dependent absorption in ATR geometry into account.[28] An electrical current (0.3 A) was sent for 4 s through a heating wire (0.26 Ohm) in the salt solution leading to a transient increase of DNA hydration through the gas phase. The ensuing IR absorption changes were measured time-dependently with a liquid nitrogen-cooled MCT detector over 40 s by rapid scan FTIR spectroscopy (resolution: 2 cm^{-1} and 3.2 s; using an IFS/66v/S spectrometer, BRUKER Optic GmbH, Karlsruhe, Germany) followed by 2.5 min for full relaxation. Series of time-resolved interferograms from 10 hydration pulses were recorded, Fourier-transformed, and co-added for each time-slice in an automated fashion using OPUS software (BRUKER Optics GmbH, Karlsruhe, Germany). Difference spectra were calculated relative to the absorption of the equilibrated film. The method is selective for only those vibrational modes that undergo hydration-specific absorption changes. Band assignments are taken from the literature.[29,30] Circular dichroism (CD) spectra were recorded with a J-815 spectrometer (JASCO, Gross-Umstadt, Germany) equipped with a continuously stirred temperature-controlled 1 cm cuvette connected to automated syringes for peptide injection.

Spectral Processing. The scissoring absorption of liquid water (1600−1700 cm^{-1}) was subtracted from the spectra. As liquid water absorbs differently from the DNA-bound water, the subtraction generates a broad residual difference band (−1690/+1635 cm^{-1}) on which signals from nucleobases (C═O and C═N stretching) become discernible as superimposed narrow structures. Absorption losses by swelling of the DNA film upon water uptake were corrected by scaling the reference spectrum to achieve zero integral absorption change. The resulting time-dependent scaling factors f correlate with the relative volume changes by $\Delta V/V = 1 - f$. Relative molar expansion coefficients $\alpha = \Delta(\Delta V/V)\,\Delta\Gamma^{-1}$ were determined as the slope of the $f(\Gamma)$ plot. 2D

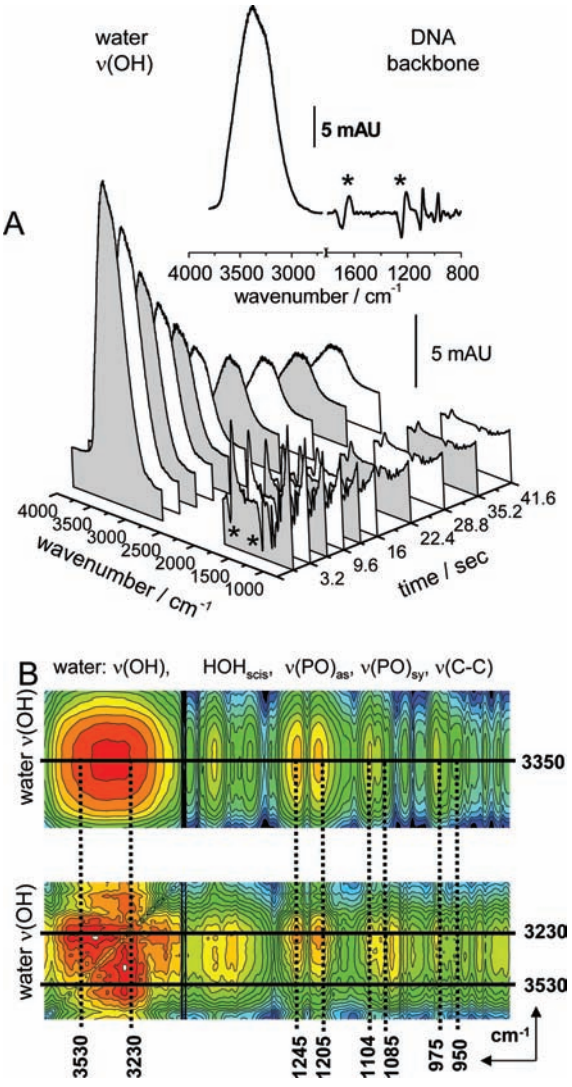

Figure 1. Acquisition and processing of hydration pulse-induced rapid scan FTIR-difference spectra. (A) IR-absorption changes after pulsed hydration (4 s) of a DNA film and their decay during re-equilibration with the gas phase. Inset: After spectral corrections (exemplified for the difference spectrum at t = 0), frequency shifts of backbone vibrations (e.g., PO_{as}, asterisk) are discernable and the water OH scissoring absorption (~1635 cm^{-1}) is replaced by a residual broad difference band (asterisk). (B) Upper panel: synchronous plot generated from 10 pulse-experiments (log scale from blue to red). Lower panel: disrelation plot revealing two water populations in the 3000−4000 cm^{-1} range with different decay kinetics. The PO_{as} amplitudes at 1245/1205 cm^{-1} have a cross peak on the 3230 cm^{-1} line and are thus not synchronized with the w_2 population but rather with w_1, leading to minimal disrelation between the 1249/1209 cm^{-1} amplitude and the 3530 cm^{-1} water ν(OH) after normalization (Figure 2D, see also Materials and Methods).

dx.doi.org/10.1021/ja108863v | J. Am. Chem. Soc. 2011, 133, 5834–5842

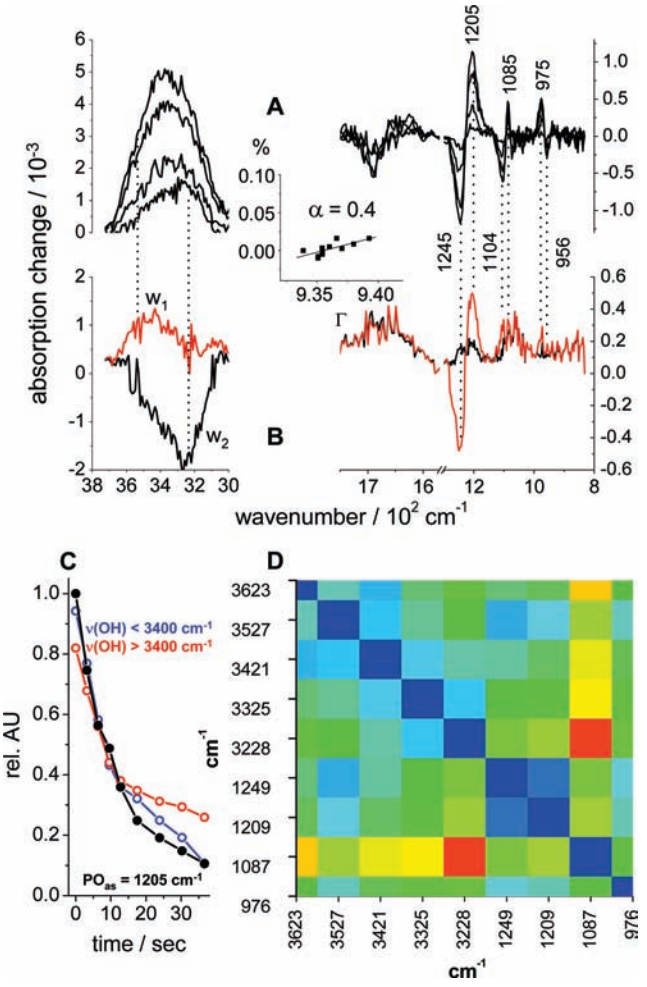

Figure 2. Hydration-induced difference spectra at Γ = 9.33. (A) The water ν(OH) absorption (3800−3000) decreases over time (1.5, 4.6, 14.2, and 38.1 s) upon release of excess water to the gas phase while H-bond changes to the DNA backbone cause frequency shifts in the 1300−800 cm^{-1} range dominated by increased H-bonding to the PO_2^- groups (down shift of the PO_{as} causes the 1245/1205 cm^{-1} difference band) but showing little B_I state formation (small changes at 1085, 1060, and 975 cm^{-1}). (B) Disrelation spectra referenced to the water ν(OH) at 3530 cm^{-1} (w_1, black) and 3230 cm^{-1} (w_2, red) showing the large kinetic similarity of the PO_{as} and the w_1 (small amplitudes) but not the w_2 absorption (large disrelation amplitudes). Inset: linear relation between water content (Γ = mol H_2O/mol DNA-phosphate) and sample expansion. The coefficient α is the slope of the linear regression line. (C) Time course of the integral high frequency (3700−3500 cm^{-1}, red) and low frequency (3400−3200 cm^{-1}, blue) half of the water ν(OH) absorption and of the PO_{as} (black). The disrelation spectra represent the root square deviation of the absorption changes from those of the ν(OH) of w_1 and w_2. (D) Disrelation map showing similarity (blue) and dissimilarity (red) of the time dependencies in pairwise comparisons of selected infrared bands. The amplitudes are normalized with respect to band intensities to represent purely kinetic dissimilarities. The w_1 ν(OH) at 3527 cm^{-1} and the PO_{as} of the B_I state (1209 cm^{-1}) are synchronized (blue square), whereas the PO_{sy} (1087 cm^{-1} in B_I) and PO_{as} modes are not.

disrelation maps were obtained from pairwise comparisons of the kinetics of absorption bands as described[31] using Origin 7.5. The plots in Figures 2−4 visualize in a concise manner the more than 30 pairwise comparisons between the relaxation kinetics of absorption changes in the water OH stretching (ν(OH)) region (3600−3000 cm^{-1}) and of the DNA backbone: asymmetric PO_2^- stretching (PO_{as}, 1220−1260 cm^{-1}), symmetric PO_2^- stretching (PO_{sy}, 1080−1090 cm^{-1}), deoxiribose C−O stretching (ν(C−O), 1050−1060 cm^{-1}), and the deoxyribose C−C stretching (ν(C−C), 960−970 cm^{-1}). The color-coded amplitude is the positive root square deviation of the time-courses at the wavenumbers labeled at the *x*- and *y*-axes. Normalization to the synchronous correlation amplitudes visualizes kinetic differences independently of band intensities. Peak frequencies deviate from those in the raw data when the kinetics differ more in the side lobes than the original absorption peak.

The measuring scheme is exemplified in Figure 1. Pulsed hydration of a DNA film causes transient IR absorption changes which decay during re-equilibration of the added water with the gas phase. The water ν(OH) and scissoring band (~1635 cm^{-1}) scale with water uptake and increase initially, whereas the DNA absorptions (e.g., by the nucleobases and the PO_{as}, labeled by asterisks) decrease due to the hydration-induced film expansion. The underlying frequency shifts become visible after spectral correction (Figure 1A, inset). Absorption of the initial state is negative, and that of the state generated by hydration is positive. The spectral changes are reversible and differences between data sets are within the noise level.

The coupling of hydration to DNA conformation is reflected by the synchronicity of the frequency shifts of the involved H-bonded donor/acceptor groups with the temporal change of the water ν(OH) absorption. Furthermore, water release after the hydration pulse is related to the DNA−water interaction strength: strongly bound water leaves its binding site at a lower partial pressure, that is, at later times. Thus, the kinetic heterogeneity of water and DNA absorption changes allows identifying the presence of disjunct water−DNA interaction sites not discernable in static spectra.

Figure 1B (upper panel) shows the synchronous correlation between the time courses of the water ν(OH) (3600−3000 cm^{-1}) and the DNA absorptions (1800−800 cm^{-1}). Because of the overall similarity of the absorption decays, similar spectral characteristics prevail along cross sections parallel to either of the wavenumber coordinates. The disrelation map (Figure 1B, lower panel) generated from the same 2D set,[31] however, identifies kinetic deviations by the splitting into weakly and strongly H-bonded water populations w_1 and w_2 absorbing at ~3530 and ~3230 cm^{-1}, respectively. The shift of the disrelation amplitude of the PO_{as} absorption change (1245/1205 cm^{-1}) toward the low frequency ν(OH) region shows that changes of the PO_2^- H-bond strength are not correlated with the w_2 population.

The kinetic deviation of all absorption changes from those of w_1 and w_2 will be presented as two disrelation spectra which show the root square deviations of the time courses from those of the ν(OH) of either w_1 or w_2. The signs of the original absorption bands are preserved (positive root) when their decay is faster than the ν(OH) reference, otherwise bands are inverted (negative root).[31] Hence, structural features that relax faster or slower than the ν(OH) of w_1 or w_2 can be identified from disrelation spectra in a model-independent manner. The normalized 2D plots, on the other hand, assess the kinetic heterogeneity of the most prominent structural changes in a single picture and easily identify cooperative transitions by their homogeneous kinetics in all absorption changes.

RESULTS

Hydration-induced difference spectra of DNA films have been recorded at selected times after an incremental growth of the HS of genomic DNA (Figure.1A) at different initial hydration levels. Besides the spectral information, the kinetics of absorption changes were analyzed by 2D correlation and relative changes in the molar volume of HS water were assessed (Materials and Methods). The assignment of spectroscopically different water

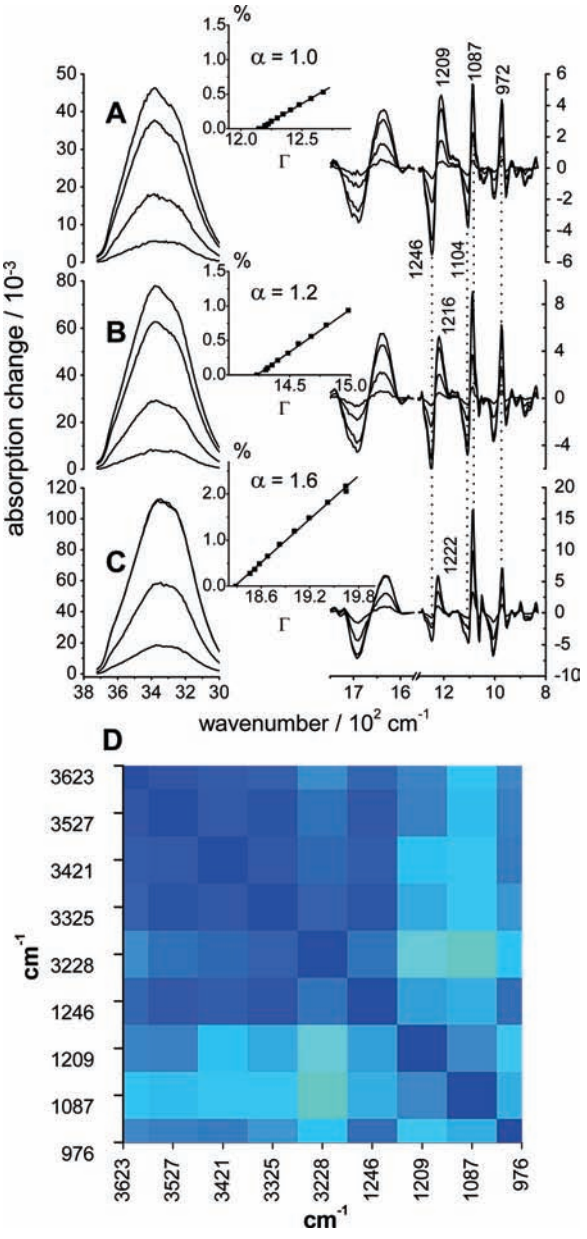

Figure 3. Hydration-induced $B_{II}-B_I$ transition as a function of basal hydration. Data are scaled to the same amount of DNA as in Figure 2 and were obtained with initial Γ of (A) 12.1, (B) 14.2, and (C) 18.3. Insets show the linear relations between Γ and % film expansion per added water molecule leading to the coefficients α which increase with basal hydration. Five representative difference spectra (1.5, 4.6, 14.2, and 38.1 s) are shown for each experiment. Note that with HS growth, the PO_{as} difference band (1200−1250 cm^{-1} range) is reduced in relation to water uptake, whereas the B_I-B_{II} transition increases (PO_{sy} 1110−1080 cm^{-1} range). (D) Disrelation map obtained with Γ = 12.1 showing the high degree of synchronicity of all infrared-spectral changes typical of a cooperative transition seen at 12 < Γ < 14.

populations to specific DNA hydration sites is aided by the kinetic analysis. "Adsorptive" and "cooperative" hydration regimes could be distinguished which differ in water packing volume and conformational coupling to the DNA backbone as described in the following. The role of these water populations in peptide recognition will be presented.

"Adsorptive" Hydration Regime. Figure 2A shows the effect of HS growth at low basal hydration. The water content increased initially from 9.33 to 9.39 water molecules per phosphate (inset), as derived from the water ν(OH) peak increase by ∼5 mAU, followed by re-equilibration of water with the gas phase and a successive reduction of the initially produced spectral changes over time. The lack of structure in the residual water HOH scissoring difference band (1700/1600 cm^{-1}, Materials and Methods) evidences the lack of nucleobase absorption changes, whereas the PO_{as} shift (1245/1205 cm^{-1}) reflects the increased H-bonding to the DNA phosphates upon water uptake. The symmetric PO_2^- stretching mode (PO_{sy}) responds weakly (1104/1085 cm^{-1}), indicative of little structural change, and the deoxyribose ν(C−C) undergoes an upshift (968/975 cm^{-1}). The disrelation spectrum in Figure 2B shows that the w_1 population is strongly correlated with the PO_{as} absorption resulting in negligible amplitudes at 1245 and 1205 cm^{-1} when compared to the 3530 cm^{-1} ν(OH), whereas a slower re-equilibration of w_2 leads to the disrelation amplitude at the PO_{as} frequency, when compared to the ν(OH) of w_2 at 3230 cm^{-1}. The implied temporal shift of the water ν(OH) in the raw data is seen as a gradual decrease of the ν(OH) peak frequency (Figure 2A) as w_2 is released slower than w_1. The stronger attachment of w_2 to the DNA agrees with its lower ν(OH) and thus stronger H-bond than w_1. Therefore, the disrelation spectra clearly show that w_2 does not interact with the PO_2^- groups which revert to their less H-bonded state while w_2 is still bound to the DNA. The IR signatures of these disjunct water populations can be seen in the ν(OH) region (Figure 2B) and are identified by the expected sign reversal, showing a positive disrelation amplitude for the high frequency ν(OH) of w_1 (red trace) when referenced against the slower w_2 absorption change, and a negative amplitude (black trace) vice versa. We assign the w_1 and w_2 absorptions to water solvating the PO_2^- groups and non-PO_2^- sites (sugars and nucleobases), respectively. This kinetic distinction is a robust feature seen directly in the time domain. Figure 2C shows the decay of the integral ν(OH) absorption at high (red) and low ν(OH) frequencies of water (blue). The high frequency ν(OH) is more synchronized with the PO_{as} absorption change (black) than the low frequency-absorbing w_2 populatio which is longer and more strongly attached to the DNA. The disrelation spectra (Figure 2B) express the corresponding root square deviation in their amplitude and sign (Materials and Methods). The PO_{as} has a large amplitude when compared to the slower relaxing w_2 absorption and its sign is preserved because it reacts faster than the reference band. Remarkably, water uptake at this low hydration level occurred with negligible film expansion (α = 0.4%, Figure 2, inset). In summary, the revealed PO_2^- hydration conforms with an adsorptive water binding mode largely uncoupled from conformational transitions and swelling.

The kinetic differences are represented independently of intrinsic band intensities, in the normalized 2D plot in Figure 2D (color-code: blue to red, fully synchronized to highly asynchronous). For example, the PO_{as} absorptions in the initial weaker H-bonded B_{II} and in the more hydrated and stronger H-bonded B_I state are highly synchronized because they originate in the same vibrational mode. Correspondingly, the amplitude at 1249/1209 cm^{-1} almost vanishes. For clarity, only the (positive) absorptions of the PO_{sy} and ν(C−C), characteristic of the formation of the B_I state, are included in the map. The plot confirms the synchronicity of the w_1 absorption at ∼3530 cm^{-1} with the PO_{as} in B_I, sampled at 1209 cm^{-1}, and reveals the low correlation of the PO_{sy} with all other absorption changes. The w_2 absorption does not reach the degree of synchronicity with any of the DNA backbone vibrations seen with w_1 but exhibits its lowest

dx.doi.org/10.1021/ja108863v | J. Am. Chem. Soc. 2011, 133, 5834–5842

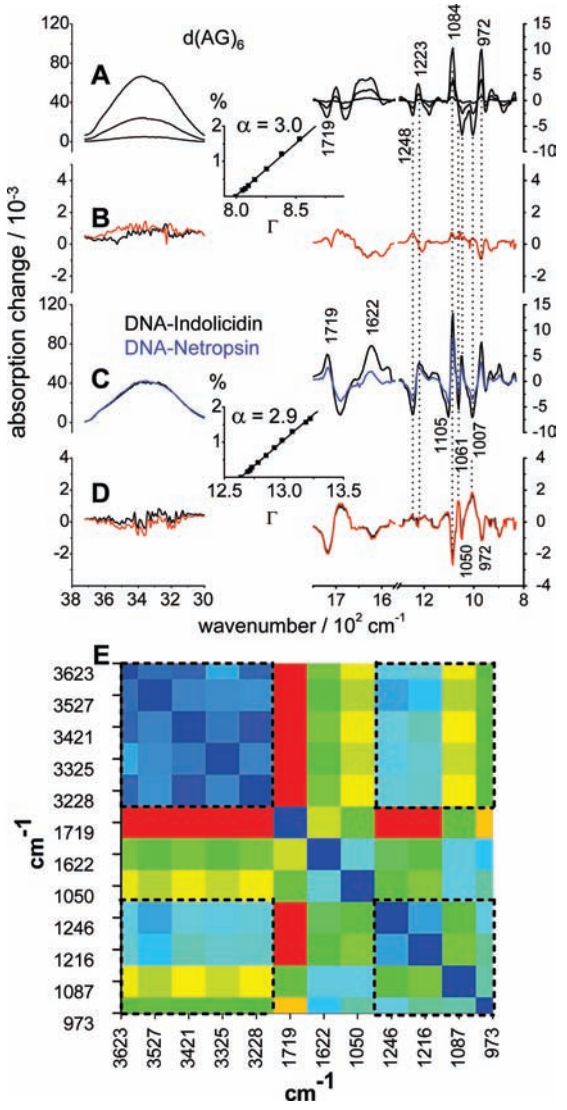

Figure 4. Hydration response of the single-strand $d(AG)_6$ and of peptide-bound ds DNA. Spectra are normalized to the same amount of DNA as in Figure 2. Five representative difference spectra (1.5, 4.6, 14.2, and 38.1 s) are shown for each experiment. (A) Hydration-induced absorption changes in $d(AG)_6$. (B) Disrelation spectra of $d(AG)_6$ (referenced against w_1 and w_2, black and red trace, respectively). (C) Hydration-induced absorption changes in dsDNA in the presence of indolicidin (black) and the minor groove binder netropsin (blue). (D) Disrelation spectra of the hydration-induced absorption changes in the presence of indolicidin (referenced against w_1 and w_2, black and red trace, respectively). Water absorption changes are kinetically homogeneous (no disrelation amplitudes in the ν(OH) range as opposed to Figure 2B). Backbone alterations lag behind the hydration modulation, leading to disrelation amplitudes that are inverted relative to the original spectra (Materials and Methods). Insets show the volume expansion as a function of Γ, resulting in the relative molar expansion coefficients α. (E) Normalized disrelation map of the absorption changes in the presence of indolicidin. Except for the PO_{as} (1246/1216 cm^{-1}), synchronicity with the hydration changes is lost for the DNA backbone absorptions. Boxed areas contain the bands present in the maps in Figures 2 and 3, whereas the absorptions at 1719, 1622, and 1050 are additionally induced only in the presence of indolicidin/netropsin.

disrelation with the ν(C−C) absorption change (~3230/975 cm^{-1} cross peak) suggesting the linkage of w_2 to the deoxyribose environment, whereas w_1 is clearly associated with the PO_2^- groups. Despite the large response of the PO_{as} to increased H-bonding upon HS growth (frequency shifts down), B_I-formation is largely blocked at this low hydration as the B_I marker bands at ~1085 cm^{-1} (PO_{sy}) and ~975 cm^{-1} (ν(C−C)) are small and that at ~1060 cm^{-1} (ν(C−O)) is absent. The B_I state is thus not directly linked to PO_2^- hydration and its correlation with the water ν(OH) absorption is low in the entire 3600−3000 cm^{-1} range (see color code along 1087 cm^{-1} line in Figure 2D).

"Cooperative" Hydration Regime. At Γ = 12.1, the PO_{sy} and ν(C−C) bands gain intensity, whereas the PO_{as} change per added water moleule is only 50% of that at Γ=9.3 (Figure 3A) due to the higher basal PO_2^- solvation which reduces the number of vacant water uptake sites. The PO_2^- and ν(C−C) modes at Γ >12 (Figure 3B,C) exhibit the typical features of the thermally induced B_{II} to B_I transition.[12] The expected reduction of additional PO_2^- H-bond formation per water molecule added to a larger HS contrasts the increase of the B_{II}−B_I transition per added water evident from the increased PO_{sy} absorption change for larger HS (Figure 3A−C). The different responses of the two PO_2^- vibrations reveal the complex nature of the two normal modes. The PO_{sy} is rather insensitive to direct H-bonding (little response at Γ = 9) but responds to the phosphodiester conformation[32] and thus accompanies the substate transition for which it constitutes an IR-spectral hallmark.[6] Vice versa, the PO_{as} senses H-bonding without being indicative of a conformational transition. Importantly, the salient property of the sample at 12 < Γ < 14 versus a smaller HS is the high cooperativity of all structural and H-bond changes resulting in negligible normalized disrelation amplitudes of both water and DNA absorptions (Figure 3D). Surprisingly, the kinetic homogeneity is contrasted by the increased ν(OH) absorption bandwidth of 418 cm^{-1}, evidencing a larger heterogeneity of water H-bonds than at low hydration (390 cm^{-1} fwhm). Therefore, the synchronicity of water and DNA absorptions reveals the modulation of a contiguous outer water layer (not present at Γ = 9) that is cooperatively linked to DNA conformation rather than saturating chemically defined and kinetically distinct binding sites as seen in the smaller HS (Γ < 12). Furthermore, the relative molar expansion coefficient α of the added water increases to 1.6% at Γ ~18 (Figure 3, insets) evidencing the formation of a "water envelope" that lowers the DNA packing density. Concomitantly, the PO_{as} frequency in the B_I state increases (compare Figures 3A−C and 2A). This reveals the weakening of the PO_2^- H-bonds of the B_I state in the more extended HS (although still stronger than in B_{II}) and agrees with the more heterogeneous water structure deduced from the ν(OH) bandwidth.

Increased water disorder in the larger HS, rather than changes in PO_2^- solvation, is thus the dominant factor in B_I formation and is confirmed by the difference spectra at elevated hydration, where the conformation-sensitive PO_{sy} and the ν(C−C) absorption changes dominate the difference spectra (Figure 3B,C) and the PO_{as} frequency in the B_I state shifts up from 1209 to 1222 cm^{-1}. The decrease of the intensity ratio of the PO_{as}/ν(C−C) absorption from 3 to 1.3 upon modulating the Γ = 9 ("inner") or the Γ = 18 ("outer") hydration layer indicates that the PO_{as} is maximally sensitive to hydration (by w_1) before the contiguous water envelope is formed. In contrast, changes at the non-PO_2^- sites (sensed by the ν(C−C)) are only transmitted through a more extended water H-bond network affecting the non-PO_2^--bound w_2.

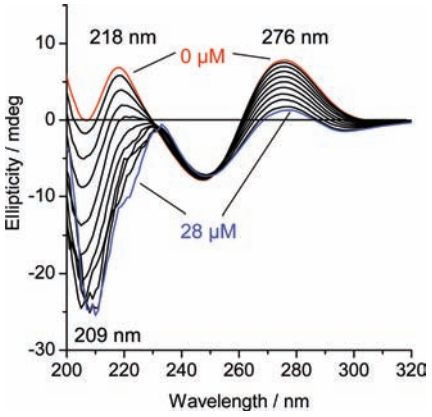

Figure 5. Titration of dsDNA with indolicidin monitored by circular dichroism. A total of 17 aliquots of 50 μL of 0.1 mM indolicidin in 10 mM NaCl were injected in 3 mL of dsDNA (0.15 mM in phosphate, 10 mM NaCl). The 209 nm band is typical of the unstructured peptide. The changes in the 250/276 nm difference band of ds DNA indicate dehydration of bases upon indolicidin binding.

Remarkably, and opposite to the w_1-PO_2^- interaction, hydration pulses always weaken the H-bonding to the deoxyribose (frequency upshift of the ν(C−C)) which can be rationalized by softening of the w_2 H-bonds to the non-PO_2^- sites in the inner hydration layer, when the extended H-bonded water network competes with these sites for H-bonding to w_2. The relative molar volume of hydration water increases up to 4 times with Γ growing from ∼9 to 19 (Figures 2 and 3, insets) indicating swelling by intermolecular water in contrast to the "adsorptive" regime.

Hydration of a Single-Stranded Oligonucleotide. To address the possible role of the DNA grooves as hydration sites for the w_2 population modulated at low hydration, we have recorded difference spectra of the single stranded (ss) oligonucleotide $d(AG)_6$ at Γ = 8 (Figure 4A). The spectra are remarkably similar to those of dsDNA at Γ > 12 with a PO_{sy}/PO_{as} ratio almost identical with that at Γ = 18. Additional bands between 1600 and 1800 cm^{-1} arise from the purine rings as expected from their water-accessibility in the unpaired state. The replacement of the sharp ν(C−O) difference band (1060/1050 cm^{-1}), usually only observed in the cooperative regime of dsDNA (Figure 3B,C), by a broad feature shows that substate geometries are well-defined only in dsDNA. The vanishing ν(OH) disrelation amplitudes (Figure 4B) reveal a homogeneous water population in ssDNA. The different H-bonding environment in $d(AG)_6$ is further reflected by α = 2.9% under conditions where dsDNA binds water essentially without expansion. Importantly, the ssDNA data show that a Γ = 8 shell is sufficient to sustain solvation of a single strand backbone in a very similar way to that of dsDNA only at Γ > 12. The absence of the w_2 population in ssDNA allows a more efficient B_I-like hydration of the DNA backbone already at low hydration. The data imply that the double strand structure creates the non-PO_2^--sites, presumably in the grooves, where interaction with w_2 opposes B_I formation. The results support the notion that structural constraints on the dsDNA backbone are weakened when the tightly H- bonded w_2 population is perturbed by engaging in additional water−water contacts in the contiguous water layer in the "cooperative" regime.

Hydration of the Indolicidin−DNA Complex. We have asked how water contributes to DNA−ligand interactions in the complex with indolicidin, a 13-mer peptide of antimicrobial activity secreted from bovine neutrophils.[25] Indolicidin has been suggested to bind to the major groove of DNA but structural information is limited.[33] Figure 4C shows the hydration-induced difference spectra of the indolicidin−DNA complex at Γ = 12. These are almost identical with those of the netropsin DNA complex used as a spectral reference for known minor groove specificity.[34] Similar to ssDNA, water induces an absorption change at 1719 cm^{-1} (C═O and C═N stretching of the bases) in the presence of the peptides which is not observed at any Γ in free dsDNA. The frequency shift is indicative of H-bond changes at guanine in the major groove.[35] Both peptides disrupt the cooperativity of the hydration-driven B_{II}−B_I transition. This is seen in the disrelation spectra of indolicidin in Figure 4D, where the H-bond-sensitive PO_{as} stays fully synchronized with the water ν(OH) absorption (small amplitude in the disrelation spectra) but is fully uncoupled from the B_I−B_{II} transition: the structure-sensitive difference bands of the DNA backbone between 1300 and 800 cm^{-1} lag behind the hydration changes and, therefore, become inverted in the disrelation spectra (Figure 4D). Despite the loss of cooperativity, the peptide promotes the water-driven B_I formation as evident from the similarity with the spectra of dsDNA at Γ=18 and from the more than 50% reduced amount of water needed per PO_2^- to evoke absorption changes of comparable size as in free dsDNA (compare ν(OH) region in Figures 3C and 4C).

The normalized disrelation plot in Figure 4E visualizes the sequence of group-specific changes in the DNA−indolicidin complex entailed by the hydration pulse in the order of decreasing synchronicity with the water ν(OH) from blue, green, yellow to red. Rows 1−5 (water ν(OH)) of columns 6−12 (DNA/peptide absorptions) in Figure 4E show that the PO_{as} is tightly coupled to hydration changes (light blue) followed by weakening of H-bonding to the sugars (ν(C−C) upshift to 973 cm^{-1}, green). The conformation-sensitive PO_{sy} (1087 cm^{-1}) and sugar ν(C−O) at 1050 cm^{-1} respond with a larger time lag (yellow), and the shift of the purine ring vibration at 1719 cm^{-1} is a late response (red). Although slower than in free dsDNA, B_I formation is more efficient, which we ascribe to the displacement of the B_{II}-stabilizing w_2 by the peptides. Local dehydration and an altered state of the nucleobases is supported by CD spectroscopy. Figure 5 shows the typical B-DNA spectrum with a 248/276 nm difference band and a zero crossing at 260 nm. The decrease of the 276 nm band and the shift of the crossing to longer wavelengths upon successive addition of indolicidin reveals base destacking and dehydration[36] in the complex, respectively.

■ DISCUSSION

We have identified by correlation analysis of rapid-scan FTIR difference-spectra the sequential steps that couple an incremental extension of differently sized HS to conformational B_I−B_{II} transitions in free and peptide-bound B-DNA. A water population w_1, which is less H-bonded than bulk water, interacts with the HS of the PO_2^--groups and exchanges with the gas phase more rapidly than the population w_2 linked to the hydration of non-PO_2^--sites by H-bonds that are stronger than in bulk water. These populations are well resolved at Γ < 12 (Figure 2) and their assignment to disjunct DNA binding sites agrees with crystallographic data revealing separated hydration spheres of PO_2^- and non- PO_2^- sites at similar hydration.[37] In this "adsorptive" regime, hydration has little effect on DNA conformation and the lack of volume expansion indicates the hydration of "concave" DNA surface regions and high water packing

dx.doi.org/10.1021/ja108863v |J. Am. Chem. Soc. 2011, 133, 5834–5842

density. The H-bond strengths and gas phase exchange kinetics of the different water populations are likely to correlate with properties assessed by other methods. It appears reasonable to assign the stronger bound w_2 population to the slowly diffusing water in DNA films measured by neutron scattering under very similar conditions,[18] whereas the other species probably represent the fast diffusing water. A similar differentiation was achieved by fluorescence spectroscopy in solution.[19,38] Since the w_2 cluster is specific for dsDNA, the lack of the 20 ps in ssDNA also strongly supports the proposed assignment and the increased ssDNA backbone solvation at lower total water content agrees with the release of water, putatively w_2, upon dsDNA melting.[4,39]

At $12 < \Gamma < 14$, hydration couples cooperatively to the $B_{II}-B_I$ transition within a contiguous water shell that favors B_I formation leading to the observed synchronicity of the $B_{II}-B_I$ transition with the modulation of the outermost hydration layer which itself has no direct contact to any of the backbone groups which are already saturated at lower hydrations than those studied here.[37] The widened ν(OH) band (418 cm^{-1} fwhm) reveals increased water−water interactions as compared to the "adsorptive" regime. Yet, the ν(OH) band is 30 cm^{-1} narrower than in liquid water evidencing an ordered H-bond network. Therefore, the water layer interrogated by pulsed hydration in this regime is in direct contact neither with DNA nor bulk water, but effectively links the DNA-bound w_1 and w_2 clusters into a contiguous HS. The larger volume change related to its modulation supports the more peripheral location. The perturbation of the non-PO_2^--bound w_2 cluster, either by increasing disorder upon HS growth or by ligand binding, promotes B_I formation and is thus crucial for substate-specific DNA recognition as discussed below.

DNA Conformation Is Linked to the Degree of Water Disorder in the Hydration Shell. The cooperative regime is clearly the most relevant to understand how DNA-bound water by itself or in concert with a ligand affects B-DNA conformation. The splitting of the w_1 and w_2 H-bond energy around that of bulk water is probably essential for this coupling. It allows merging of both populations into a water envelope of bulk-like average H-bond strength at little enthalpic cost and the required transitions of the individual water molecules are thermally accessible as the H-bond imbalance is 3−4 kJ mol^{-1} (corresponding to the measured $\Delta\nu$(OH) of ∼300 cm^{-1}). Thereby, ideal conditions are met to generate an extended nonrandom H-bond network that nevertheless matches the H-bond strength of liquid water resulting in a "smooth" isoenthalpic connection to the bulk phase. In this regime, HS growth populates the B_I state via the replacement of the B_{II}-stabilizing DNA−w_2 interactions in the inner shell by water−w_2 interactions within the water envelope. The IR-data suggest a functional role of the previously identified extended water networks[40,41] in connecting DNA conformation to hydration distant from the DNA surface. Importantly, the results show that this linkage is based on increasing disorder in the more tightly bound water (w_2) at nonphosphate sites, rather than inducing structure through any site-specific binding.

The B_{II}-stabilizing function of the non-PO_2^--bound water agrees with the proposed migration of water from the PO_2^- to the phosphodiester and sugar moieties during B_{II} formation in the glassy state.[6] This mechanism is supported here only at low hydration, where the PO_{as} difference band decays not only faster than w_2 (Figure 2B,C), but also faster than the integral water ν(OH) absorption (not shown), demonstrating that water leaves the PO_2^- groups before it is released from the DNA to the gas phase (Figure 2 C). However, the PO_{as} absorption is not generally synchronized with the $B_{II}-B_I$ transition and a large PO_{as} response correlates with little

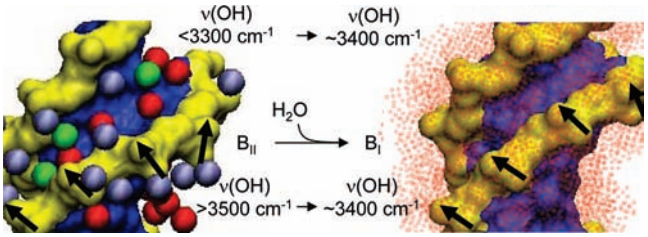

Figure 6. Relation of spectroscopically identified water clusters to structurally resolved hydration sites. Left: Crystallographically resolved water oxygens are labeled red (minor groove), gray (PO_2^--bound), and green (intermediate locations). The orientation of the O_1-O_2 connector at PO_2^--groups (arrows) indicates the presence of three PO_2^--groups in the B_I and one in the B_{II} state (coordinates: 1HQ7). The ν(OH) frequencies of w_1 and w_2 are placed at the proposed sites where they extend the inner HS. Right: Growth into a contiguous HS relieves the B_{II}-stabilizing constraints, exerted to a large extent by the structured water network linked to the minor groove. The homogeneous nonrandom water envelope (symbolized by dotted surface) exhibits bulk-like average H-bond strength and promotes the B_I state (arrows) by weakening w_2 H-bonds and enforcing PO_2^- H-bonds, resulting in an essentially isoenthalpic transition.

B_I formation (and vice versa, see Figures 2 and 3, respectively). This discrepancy with low temperature FTIR spectra is probably due to the uncoupling of hydration dynamics from conformational dynamics during quick-freezing of DNA.[12] Under these conditions, an additional absorption change at 1719 cm^{-1} (C═O and C═N stretching of nucleobases) was attributed to base stacking changes which have been suggested to accompany the B_I-B_{II} transition.[8,42] We have shown here that, at ambient temperature, water-induced absorption changes in dsDNA above 1700 cm^{-1} are almost negligible (Figure 3C). The correlation of base stacking with DNA−water interactions has also not been supported by MD calculations.[43] Our data show that the $B_{II}-B_I$ transition is controlled by the degree of disorder in the nonphosphate-bound water. Figure 6 summarizes the relation of the spectroscopically identified water clusters to crystallographically resolved hydration sites and their implication in the B_I-B_{II} transition.

Release of Nonphosphate-Bound Water Mediates Structural Preference in DNA Recognition by "Unstructured" Peptides. Indolicidin replaces water from the DNA hydration shell and favors the B_I state with spectral properties almost indistinguishable from those caused by netropsin, suggesting that also indolicidin binds to the minor groove of DNA. Remarkably, B_I formation in both complexes still depends on hydration: the difference bands in Figure 4C occur because the peptides by themselves do not arrest the DNA in the B_I state. Instead, hydration promotes B_I formation of the entire complex, supporting the notion of a water-dependent induced fit. The 1622 cm^{-1} difference band (tentatively amide I), absent in pure dsDNA, may indicate the accompanying peptide conformational changes. We ascribe the enhanced B_I formation to the specific displacement of the tightly bound w_2 which is presumably connected to the "hydration spine"[44] in the minor groove. We have shown that B_I formation itself is not linked to base stacking changes. The B_I conformation may, however, facilitate the transition to unstacked states (characterized by the 1719 cm^{-1} absorption) which interact favorably with the peptides. This is supported by the sequential (B_I forms before stacking alteration) rather than concerted transition in the DNA−indolicidin complex (Figure 4D,E).

Intriguingly, the results imply that net hydration causes DNA dehydration at the indolicidin binding site. Dehydration during

biomolecular recognition is typically linked to entropy gain when interfacial water is released to the solvent. This is predominant for minor groove binders[45,46] and has been ascribed to the highly ordered structure and more strongly bound minor groove water.[47] In line with these calorimetric estimates, we have shown here by the differences in ν(OH) and gas phase re-equilibration rates that indeed the groove-bound water exhibits stronger H-bonds than both bulk water and the water molecules that extend the core PO_2^--solvation shell (present at all basal hydration levels studied here), supporting a high entropic gain upon its release at high enthalpic cost. Since the DNA-films studied here are not immersed in a bulk phase, water displaced from the netropsin-binding interface upon hydration can only relocate to other hydration sites (as it can also not be released to the gas phase during the net water uptake). In fact, water relocation explains the larger PO_2^- response in the DNA netropsin complexes produced by less water uptake than in free DNA (Figures 3C and 4C). Also the upshift of the PO_{as} frequency in the B_I form of the DNA peptide complexes (1223 cm^{-1}, Figure 4C) agrees with the relocation of interfacial water to increase solvation of the PO_2^--groups, because the frequency of this mode correlates with HS size (Figure 3) and is found in the complex at $\Gamma = 12$ at a position typical of $\Gamma > 14$. The synchronous response of the PO_{as} to hydration (Figure 4D,E) further evidences unhindered access of water to the PO_2^- groups in agreement with the peptide displacing w_2, rather than the PO_2^--bound w_1. Similar to a bulk water phase, the growth of the more disordered and less H-bonded PO_2^--associated water probably provides the H-bond network that supports the gain of entropy for the released interfacial water. This underscores the crucial role of the number of accessible H-bonded states within the HS in defining how inner shell water will couple to the B_I-B_{II} equilibrium upon perturbation of more distant water layers of the HS.

CONCLUSIONS

The B-DNA conformation couples to the aqueous phase through an extended nonrandom H-bond network of bulk-like average H-bond strength. Upon HS growth, the water layer is restructured at little enthalpic cost as H-bond imbalances at disjunct DNA hydration sites become equalized. The increasing number of water−water contacts relieves the B_{II}-stabilizing water−DNA constraints at the non-PO_2^- sites. The B_I state is thus populated by the decrease of order in the growing HS, rather than by saturation of B_I-specific hydration-sites. Indolicidin displaces the B_{II}-stabilizing water and couples hydration efficiently to the B_I-formation almost indistinguishably from the minor groove binder netropsin. A sequential induced fit is initiated by PO_2^- solvation, followed by B_I formation and ultimately leads to peptide-induced stacking changes of the nucleobases. Abolishing B_{II}-stabilizing water−DNA interactions at non-PO_2^- sites either by linkage to an extended less ordered water network or by peptide-induced water displacement confers substate specificity to both processes.

AUTHOR INFORMATION

Corresponding Author
k.fahmy@hzdr.de

REFERENCES

(1) Dickerson, R. E.; Drew, H. R.; Conner, B. N.; Wing, R. M.; Fratini, A. V.; Kopka, M. L. *Science* **1982**, *216*, 475–85.
(2) Ghosh, A.; Bansal, M. *Acta Crystallogr., Sect. D: Biol. Crystallogr.* **2003**, *59*, 620–6.
(3) Fuller, W.; Forsyth, T.; Mahendrasingam, A. *Philos. Trans. R. Soc., B* **2004**, *359*, 1237−47; discussion 1247−8.
(4) Mrevlishvili, G. M.; Carvalho, A. P. S. M. C.; Ribeiro da Silva, M. A. V.; Mdzinarashvili, T. D.; Razmadze, G. Z.; Tarielashvili, T. O. *J. Therm. Anal. Calorim* **2001**, *66*, 133–44.
(5) Banyay, M.; Graslund, A. *J. Mol. Biol.* **2002**, *324*, 667–76.
(6) Pichler, A.; Rudisser, S.; Mitterbock, M.; Huber, C. G.; Winger, R. H.; Liedl, K. R.; Hallbrucker, A.; Mayer, E. *Biophys. J.* **1999**, *77*, 398–409.
(7) Fratini, A. V.; Kopka, M. L.; Drew, H. R.; Dickerson, R. E. *J. Biol. Chem.* **1982**, *257*, 14686–707.
(8) Grzeskowiak, K.; Yanagi, K.; Prive, G. G.; Dickerson, R. E. *J. Biol. Chem.* **1991**, *266*, 8861–83.
(9) Hartmann, B.; Piazzola, D.; Lavery, R. *Nucleic Acids Res.* **1993**, *21*, 561–8.
(10) Dickerson, R. E.; Goodsell, D. S.; Kopka, M. L.; Pjura, P. E. *J. Biomol. Struct. Dyn.* **1987**, *5*, 557–79.
(11) Taillandier, E. *Nucleic Acid Conformations Studied by Vibrational Spectroscopy*; Adenine Press: Schenectady, NY, 1990; Vol. 3.
(12) Pichler, A.; Rudisser, S.; Rauch, C.; Flader, W.; Wellenzohn, B.; Winger, R. H.; Liedl, K. R.; Hallbrucker, A.; Mayer, E. *J. Phys. Chem. B* **2002**, *106*, 3263–74.
(13) Locasale, J. W.; Napoli, A. A.; Chen, S.; Berman, H. M.; Lawson, C. L. *J. Mol. Biol.* **2009**, *386*, 1054–65.
(14) Araúzo-Bravo, M. J.; Fujii, S.; Kono, H.; Ahmad, S.; Sarai, A. *J. Am. Chem. Soc.* **2005**, *127*, 16074–89.
(15) Nguyen, B.; Neidle, S.; Wilson, W. D. *Acc. Chem. Res.* **2009**, *42*, 11–21.
(16) Maris, A. E.; Kaczor-Grzeskowiak, M.; Ma, Z.; Kopka, M. L.; Gunsalus, R. P.; Dickerson, R. E. *Biochemistry* **2005**, *44*, 14538–52.
(17) Wellenzohn, B.; Flader, W.; Winger, R. H.; Hallbrucker, A.; Mayer, E.; Liedl, K. R. *Biochemistry* **2002**, *41*, 4088–95.
(18) Bastos, M.; Castro, V.; Mrevlishvili, G.; Teixeira, J. *Biophys. J.* **2004**, *86*, 3822–7.
(19) Pal, S. K.; Zhao, L.; Zewail, A. H. *Proc. Natl. Acad. Sci. U.S.A.* **2003**, *100*, 8113–8.
(20) Huang, J. T.; Chen, Y. C.; Chang, J. C.; Jeng, K. C.; Kao, K. K.; Yang, R. C.; Kan, L. S.; Wey, M. T.; Waring, M. J.; Chen, C. S.; Chien, W. J.; Sheh, L. *Bioorg. Med. Chem.* 2010, *18*, 2575–85.
(21) Saccardo, P.; Villaverde, A.; Gonzalez-Montalban, N. *Biotechnol. Adv.* **2009**, *27*, 432–8.
(22) Jayaram, B.; Jain, T. *Annu. Rev. Biophys. Biomol. Struct.* **2004**, *33*, 343–61.
(23) Rohs, R.; Jin, X.; West, S. M.; Joshi, R.; Honig, B.; Mann, R. S. *Annu. Rev. Biochem.* **2010**, *79*, 233–69.
(24) Neumann, T.; Gajria, S.; Bouxsein, N. F.; Jaeger, L.; Tirrell, M. *J. Am. Chem. Soc.* **2010**, *132*, 7025–37.
(25) Selsted, M. E.; Novotny, M. J.; Morris, W. L.; Tang, Y. Q.; Smith, W.; Cullor, J. S. *J. Biol. Chem.* **1992**, *267*, 4292–5.
(26) Rockland, L. B. *Anal. Chem.* **1960**, *32*, 1375–6.
(27) Falk, M.; Poole, A. G.; Goymour, C. G. *Can. J. Chem.* **1970**, *48*, 1536–9.
(28) Goormaghtigh, E.; Raussens, V.; Ruysschaert, J. M. *Biochim. Biophys. Acta* **1999**, *1422*, 105–85.
(29) Taillandier, E.; Liquier, J. *Methods Enzymol.* **1992**, *211* 307–35.
(30) Banyay, M.; Sarkar, M.; Graslund, A. *Biophys. Chem.* **2003**, *104*, 477–88.
(31) Noda, I.; Ozaki, Y. *Two-Dimensional Correlation Spectroscopy Applications in Vibrational and Optical Spectroscopy*; John Wiley & Sons Ltd.: Chichester, West Sussex, England, 2004.
(32) Guan, Y.; Thomas, G. J., Jr. *Biophys. J.* **1996**, *71*, 2802–14.
(33) Hsu, C. H.; Chen, C.; Jou, M. L.; Lee, A. Y.; Lin, Y. C.; Yu, Y. P.; Huang, W. T.; Wu, S. H. *Nucleic Acids Res.* **2005**, *33*, 4053–64.
(34) Kopka, M. L.; Yoon, C.; Goodsell, D.; Pjura, P.; Dickerson, R. E. *J. Mol. Biol.* **1985**, *183*, 553–63.
(35) Ouameur, A. A.; Tajmir-Riahi, H. A. *J. Biol. Chem.* **2004**, *279*, 42041–54.

(36) Gray, D. M.; Ratliff, R. L.; Vaughan, M. R. *Methods Enzymol.* **1992**, *211*, 389–406.
(37) Schneider, B.; Patel, K.; Berman, H. M. *Biophys. J.* **1998**, *75*, 2422–34.
(38) Sen, S.; Andreatta, D.; Ponomarev, S. Y.; Beveridge, D. L.; Berg, M. A. *J. Am. Chem. Soc.* **2009**, *131*, 1724–35.
(39) Spink, C. H.; Chaires, J. B. *Biochemistry* **1999**, *38*, 496–508.
(40) Shui, X.; Sines, C. C.; McFail-Isom, L.; VanDerveer, D.; Williams, L. D. *Biochemistry* **1998**, *37*, 16877–87.
(41) Arai, S.; Chatake, T.; Ohhara, T.; Kurihara, K.; Tanaka, I.; Suzuki, N.; Fujimoto, Z.; Mizuno, H.; Niimura, N. *Nucleic Acids Res.* **2005**, *33*, 3017–24.
(42) Flader, W.; Wellenzohn, B.; Winger, R. H.; Hallbrucker, A.; Mayer, E.; Liedl, K. R. *J. Phys. Chem. B* **2001**, *105*, 10379–87.
(43) Yonetani, Y.; Kono, H. *Biophys. J.* **2009**, *97*, 1138–47.
(44) Liepinsh, E.; Otting, G.; Wuthrich, K. *Nucleic Acids Res.* **1992**, *20*, 6549–53.
(45) Privalov, P. L.; Dragan, A. I.; Crane-Robinson, C. *Trends Biochem. Sci.* **2009**, *34*, 464–70.
(46) Bouvier, B.; Lavery, R. *J. Am. Chem. Soc.* **2009**, *131*, 9864–5.
(47) Privalov, P. L.; Dragan, A. I.; Crane-Robinson, C.; Breslauer, K. J.; Remeta, D. P.; Minetti, C. A. *J. Mol. Biol.* **2007**, *365*, 1–9.